Available online at www.sciencedirect.com
SCIENCE DIRECT®
International Journal of Thermal Sciences 44 (2005) 43–52
International Journal of Thermal Sciences
www.elsevier.com/locate/ijts

Study of natural convection heat transfer in a finned horizontal fluid layer

Eric Arquis [a,*], Mohamed Rady [b,1]

[a] *TREFLE-ENSCPB, université Bordeaux I, 16, avenue Pey Berland, 33607 Pessac cedex, France*
[b] *Dept. of Mech. Engg. Technology, Benha High Institute of Technology, Benha 13 512, Egypt*

Received 10 September 2003; received in revised form 16 February 2004; accepted 22 April 2004

Available online 20 July 2004

Abstract

Numerical experiments have been carried out to investigate natural convection heat transfer and fluid flow characteristics from a horizontal fluid layer with finned bottom surface. The effects of fin height and fin spacing have been investigated for a sufficiently wide range of Rayleigh number. Quantitative comparisons of heat transfer rates and finned surface effectiveness have been reported. The insertion of heat conducting fins has been found to induce an upward fluid motion along the fin walls. For a given value of fin spacing, the number of convection cells between two adjacent fins is function of the values of fin height and Rayleigh number. In comparison with a bare plate, the heat transfer rates for low values of fin height may be decreased by the insertion of fins. For high values of fin height, the finned surface effectiveness is greater than one for a wide range of fin spacing. For low values of Rayleigh number and high values of fin height, the finned surface effectiveness increases linearly with the decrease of fin spacing. Useful guidelines have been suggested to enhance the heat transfer rates from the finned surface.

Keywords: Natural convection; Fins; Heat transfer; Effectiveness; Rayleigh–Bénard

1. Introduction

Natural convection heat transfer from finned surfaces has been the subject of a large number of both experimental and theoretical investigations. Compared to a bare plate, a finned surface increases the heat transfer area. However, with the fins, the flow rate is reduced. Thus, if not properly designed it is possible that no improvement is achieved in terms of the overall heat transfer rates. Therefore, careful design of fin arrays is necessary to improve the overall heat transfer and optimise the finned surface effectiveness.

One of the earliest studies in this field is that of Starner and McManus [1] who presented free convection data for four different rectangular fin arrays attached to a vertical, 45 degrees, and a horizontal plate. A similar experimental study has been carried out by Welling and Wooldridge [2]. They reported optimum values of fin height to spacing for maximum heat transfer from rectangular fin arrays. The flow pattern associated with free convection heat transfer from horizontal fin arrays has been also investigated by Harahap and McManus [3]. Jones and Smith [4] studied the variation of local heat transfer coefficient for isothermal vertical fin arrays on a horizontal base. Simplified design correlations and optimum arrangement for maximum heat transfer have been suggested. Other studies on the heat transfer performance of such fin configurations have been also reported [5,6].

Research interests in this field are continuous. They are recently motivated by the advance in electronics technology and the need for efficient cooling techniques. Most recently, Yüncü and Anbar [7] and Güvenc and Yüncü [8] have reported experimental studies on natural convection heat transfer of rectangular fins attached to horizontal or vertical surfaces. The separate roles of fin height, fin spacing, and fin base to ambient temperature difference have been investigated. It has been found that, for a given fin base to ambient temperature difference, the convection heat transfer rate from fin arrays takes on a maximum value as a function of fin spacing and fin height. Also, for fin arrays of the same geometry, higher heat transfer enhancement rates have been obtained with vertically oriented bases than with horizontally oriented ones.

* Corresponding author.
E-mail address: arquis@enscpb.fr (E. Arquis).
[1] Current position: Visiting professor, TREFLE-ENSCPB.

1290-0729/$ – see front matter
doi:10.1016/j.ijthermalsci.2004.04.011

Nomenclature

c	specific heat	$J \cdot kg^{-1} \cdot K^{-1}$	
g	acceleration due to gravity	$m \cdot s^{-2}$	
H	layer height	m	
h	heat transfer coefficient	$W \cdot m^{-2} \cdot K^{-1}$	
K	permeability	m^2	
k	thermal conductivity	$W \cdot m^{-1} \cdot K^{-1}$	
L	fin height	m	
M	number of control volumes in y direction		
N	number of control volumes in x direction		
NS	number of control volumes used to represent the fin thickness		
n	iteration number		
N_f	number of fins		
Nu	Nusselt number		
p	pressure	Pa	
Pr	Prandtl number		
Q	heat transfer rate	W	
Ra	Rayleigh number, $= g\beta(T_H - T_C)H^3/\nu\alpha$		
S	fin spacing	m	
T	temperature	°C	
t_f	fin thickness	m	
u, v	velocity components	$m \cdot s^{-1}$	
W	layer width	m	
x, y	Cartesian coordinates	m	

Greek symbols

α	thermal diffusivity	$m^2 \cdot s^{-1}$
β	coefficient of thermal expansion	K^{-1}
ε_f	finned surface effectiveness	
ν	kinematic viscosity	$m^2 \cdot s^{-1}$
ρ	density	$kg \cdot m^{-3}$

Subscripts

a	air
C	cold plate
E	east node
e	east face of control volume
f	fin
H	hot plate
P	control volume central node
$*$	in the presence of fins

Most of the above mentioned studies have been concerned with rectangular fins attached to vertical or horizontal bases in a free environment. Investigations with arrays of rectangular fins on horizontal or vertical surfaces in a limited and/or confined spaces, as would be likely encountered in electronic cooling systems, are rather limited. The heat transfer and fluid flow phenomena associated with vertical fins in a bottom heated fluid layer are related to the Rayleigh–Bénard convection process that arises in a horizontal fluid layer. A large amount of research work on this form of convection has been reported in the literature. In particular, much effort has been dedicated to investigate both flow-instabilities and flow-transitions or bifurcations. A general well-known result obtained by many researchers is that the first bifurcation from motionless conduction to steady-state convection occurs as the Rayleigh number is increased beyond a critical value which depends on the aspect ratio of the enclosure (see, for example, Raithby and Holland [9]).

As the Rayleigh number is further increased, the motion becomes unstable and subsequent flow-transitions lead to an increasing spatio-temporal complexity which ultimately results in turbulence. According to a typical bifurcation sequence [10–12], steady state convection becomes at first oscillatory, then turning into quasi-periodic and eventually chaotic motion. Detailed surveys of Rayleigh–Bénard convection, as well as reviews on the several studies conducted are widely available in the open literature [13,14].

On the other hand, studies on enhancement of natural convection heat transfer in a horizontal fluid layer have received very little attention. Most recently, an experimental study has been carried out by Inada et al. [15] to investigate the effects of vertical fins on the local heat transfer in a horizontal fluid layer of finite extent. The heat transfer rates have been reported for a single value of fin height and for limited values of Rayleigh number and fin spacing. To the best of our knowledge, there are no detailed parametric studies on the heat transfer and fluid flow characteristics within a finned horizontal fluid layer. The results of such studies are useful for improving the heat transfer performance of the finned surface and developing practical design guidelines.

In the present work, detailed numerical experiments have been carried out to investigate heat transfer and fluid flow characteristics from a horizontal fluid layer with finned bottom surface. The effects of fin height and fin spacing have been investigated for a sufficiently wide range of Rayleigh number. Quantitative comparisons of heat transfer rates and finned surface effectiveness have been reported.

2. Physical models

Schematic drawings of the physical models under investigation are shown in Fig. 1. The basic reference physical model is a horizontal air layer of height H and width W. The bottom plate is kept at a constant temperature T_H, while the top plate is maintained at a lower temperature T_C. The thickness of the air layer is small in comparison to the expanse of its surface. Therefore, the air will tend to circulate in a series of cells known as Bénard cells. For an infinite horizontal fluid layer, this cellular convection takes place for values of Rayleigh number greater than 1700 [9,14].

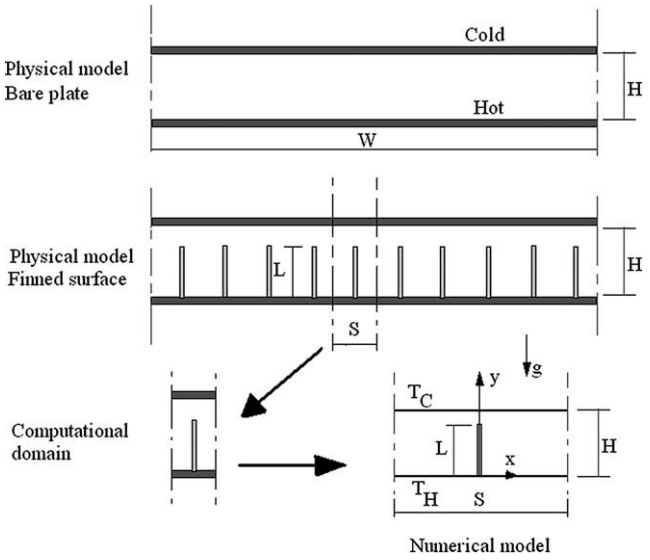

Fig. 1. Schematic drawing of the physical models and computational domain.

Heat conducting fins of thickness t_f, height L, and spacing S are now attached to the bottom plate. The objective of numerical simulations is to investigate the effects of these heat conducting fins on the heat transfer and fluid flow characteristics. Results of heat transfer and fluid flow from the finned surface are to be compared with the base case of bare plate. A two-dimensional computational domain comprising one single fin is selected for numerical simulations as shown in Fig. 1.

3. Governing equations

In the present numerical model, the heat conducting fins are considered as a part of the computational domain. Heat transfer is taking place by natural convection in the fluid layer and by heat conduction in the solid fin. This phenomenon represents a conjugate heat transfer problem. A single set of governing conservation equations, valid for the whole domain comprising the solid fins and the surrounding fluid, are written in Cartesian coordinates as:
Continuity:

$$\frac{\partial u}{\partial x}+\frac{\partial v}{\partial y}=0 \tag{1}$$

X-momentum:

$$\rho\left(\frac{\partial u}{\partial t}+u\frac{\partial u}{\partial x}+v\frac{\partial u}{\partial y}\right) = \mu\left(\frac{\partial^2 u}{\partial x^2}+\frac{\partial^2 u}{\partial y^2}\right)-\frac{\partial p}{\partial x}-\frac{\mu}{K}u \tag{2}$$

Y-momentum:

$$\rho\left(\frac{\partial v}{\partial t}+u\frac{\partial v}{\partial x}+v\frac{\partial v}{\partial y}\right) = \mu\left(\frac{\partial^2 v}{\partial x^2}+\frac{\partial^2 v}{\partial y^2}\right)-\frac{\partial p}{\partial y}-\frac{\mu}{K}v+\rho g\beta(T-T_0) \tag{3}$$

Energy:

$$\rho c\left(\frac{\partial T}{\partial t}+u\frac{\partial T}{\partial x}+v\frac{\partial T}{\partial y}\right) = \frac{\partial}{\partial x}\left(k\frac{\partial T}{\partial x}\right)+\frac{\partial}{\partial y}\left(k\frac{\partial T}{\partial y}\right) \tag{4}$$

The assumptions employed in the governing equations are in agreement with laminar incompressible flow. Appropriate spatial values of constant physical properties (density, thermal conductivity, specific heat, and viscosity) are assigned to the fluid and solid regions. Boussinesq approximation has been adopted by considering the variation of fluid density with temperature in the buoyancy driving force.

It should be observed that, the third term on the right-hand side of the momentum equations, Eqs. (2) and (3), represents the Darcy's drag force that is well known for modelling fluid flow in porous media. This term is introduced here to accommodate the presence of solid fin protrusions within the whole domain. These solid protrusions are treated as a porous media with a very low permeability (K) in comparison with the infinite permeability of the surrounding fluid. The low value of permeability in the solid region ensures an impermeable condition with zero velocity. The governing equations for the solid region, Eqs. (1)–(4), are thus reduced to the classical heat conduction equation. This technique is similar to the blocking-off method introduced by Patankar [16] to handle conjugate heat transfer problems.

The adoption of this technique requires no explicit boundary conditions to be specified at the fluid–solid interface. Thus, the boundary conditions for both the velocity and temperature fields can easily be supplied at the outer surfaces of the calculation domain. In the present study, the top and bottom walls of the computational domain have been considered impermeable with constant cold and hot temperatures, respectively. Symmetry conditions have been employed on the left and right boundaries of the computational domain. These boundary conditions can be expressed mathematically as follows:

- For the top wall ($y=H$): $u=v=0$, $T=T_C$.
- For the bottom plate ($y=0$): $u=v=0$, $T=T_H$.
- For the left and right boundaries ($x=-S/2,+S/2$): $u=0$, $\frac{\partial v}{\partial x}=0$, $\frac{\partial T}{\partial x}=0$.

4. Heat transfer rates

For a horizontal fluid layer of width W and height H, the steady state total heat transfer rate through the fluid layer at the hot (Q_H) and cold (Q_C) plates are equal. They are calculated as:

$$Q_C = Q_H = Q = \int_{-W/2}^{+W/2} -k\frac{\partial T}{\partial y}\Big|_{y=0} \mathrm{d}x$$

$$= \int_{-W/2}^{+W/2} -k\frac{\partial T}{\partial y}\Big|_{y=H} \mathrm{d}x = hW(T_H - T_C) \tag{5}$$

Where h is the average heat transfer coefficient due to natural convection. The average value of heat transfer Nusselt number based on the layer height H can be evaluated from Eq. (5) as follows:

$$Nu = \frac{hH}{k_a} = \frac{QH}{W(T_H - T_C)k_a} \tag{6}$$

Now, when the layer is equipped with fins of spacing S, the heat transfer rates from single fin spacing due to heat conduction in the solid fin and natural convection in the fluid space is given by:

$$Q_C^* = Q_H^* = Q^* = \int_{-S/2}^{+S/2} -k\frac{\partial T}{\partial y}\Big|_{y=0} \mathrm{d}x$$

$$= \int_{-S/2}^{+S/2} -k\frac{\partial T}{\partial y}\Big|_{y=H} \mathrm{d}x = h^* S(T_H - T_C) \tag{7}$$

$$Nu^* = \frac{h^* H}{k_a} = \frac{Q^* H}{S(T_H - T_C)k_a} \tag{8}$$

The effectiveness of the finned surface (ε_f) is a measure of heat transfer enhancement using fins. It is defined as the ratio of the total heat transfer rate from the finned surface to the total heat transfer rate in the absence of fins. It is calculated as:

$$\varepsilon_f = \frac{Q^* \cdot N_f}{Q} = \frac{h^* S(T_H - T_C) \cdot N_f}{hW(T_H - T_C)} \tag{9}$$

Where N_f is the total number of fins in the layer width W. For fins of negligible thickness, $N_f = W/S$, ε_f can be written as:

$$\varepsilon_f = \frac{Nu^*}{Nu} \tag{10}$$

For a particular fluid of a given value of Prandtl number, the effectiveness of the finned surface is function of the values of Rayleigh number Ra, fin length L, fin thickness t_f, and fin spacing S.

5. Numerical solution

The governing equations have been discritized using the control volume based finite difference formulation with implicit time integration [16]. The computational domain has been divided into a large number of control volumes. A sufficient number of control volumes have been positioned inside the solid region. The grid is designed such that the fin surfaces coincide with the control volumes faces passing through the solid boundaries. This allows appropriate assignment of the values of density, specific heat, viscosity, thermal conductivity, and permeability at the central nodes of both the solid and liquid computational cells. The diffusion coefficients (viscosity and thermal conductivity) at the faces of the control volumes have been calculated as the harmonic mean of their respective known values at the central nodes [16]. For example, using a uniform grid, the value of thermal conductivity at the east face of a control volume is calculated as $k_e = \frac{2k_P k_E}{k_P + k_E}$. The adoption of harmonic mean practice ensures the continuity of diffusive fluxes at the control volume faces and correctly handles the large step change in the diffusion coefficients at the solid–liquid interface [16].

The governing equations have been solved using Aquilon CFD code developed at TREFLE [17]. Solution of Navier–Stokes equations have been carried out using the augmented Lagrangian method [18]. Hybrid scheme has been chosen for discretization of the convective–diffusive transport terms [16]. The discrete algebraic equations have been solved using a preconditioned conjugate gradient method BI-CGSTAB. Steady state numerical solutions have been obtained by retaining the transient terms in the governing equations. This technique provides a kind of underrelaxation and improves the convergence to steady state solutions [16]. The code is thoroughly validated by comparisons with bench mark numerical and experimental results for fundamental CFD test cases including: natural convection in cavities, Rayleigh–Bénard convection, flow over a backward facing step, flow around a cylinder, and many others [17].

Calculations are terminated, steady state is considered satisfied, when the normalized differences in the values of temperature and velocities between two successive iterations in time n and $n + 1$ are less than 10^{-10}. The value of the normalized mass imbalance, residual of the continuity equation, is less than 10^{-12}. These criteria have been found sufficient to ensure accurate results of steady state temperature and velocity fields. The difference in Nusselt number value between two successive iterations at steady state is less than 10^{-6}. The values of Q_H and Q_C have been observed to be exactly equal at steady state. This indicates an excellent overall heat balance.

6. Results and discussion

In the present study, numerical experiments have been carried out using air $Pr = 0.71$, for six different values of Rayleigh number in the range of $Ra = (2 \times 10^3 – 3 \times 10^4)$, three different values of fin length to layer height ratio $L/H = (0.25, 0.5, 0.75)$, and nine different values of fin spacing in the range of $H/S = (0.125–2.0)$. Calculations have been carried out using high conducting (copper, $k = 200\ \mathrm{W{\cdot}m^{-1}{\cdot}K^{-1}}$) thin fins ($t_f/H = 0.05$).

A grid refinement study has been carried out to determine the effect of grid size ($N \cdot M$) on the accuracy of numerical solution. The variation of the steady state average value of Nusselt number, in the absence of fins, with grid size for a typical test case is shown in Table 1(a). It can be observed that, the difference in the calculated value of *Nu* using 100×50 and 200×100 is less than 0.5%. In the presence of fins, the sensitivity of numerical results to the number of control volumes used to represent the fin thickness (*NS*) has been examined. It can be observed from Table 1(b) that, for a grid size of $(N \cdot M) = 100 \times 50$, the difference in Nusselt number values using $NS = 10$, 6, 4, 2, 1 is within $\pm 0.15\%$. This can be attributed as due to the dominating one-dimensional heat conduction along the thin fin length that can be accurately represented using a small number of grid points along the fin width. Based on the grid refinement results, a uniform 200×100 grid with a minimum of 4 nodal points within the fin thickness has been employed in all the numerical simulations of the present study.

The results of heat transfer and fluid flow patterns for different test cases are presented in the following sections. The steady state isotherms and streamlines are discussed. In addition, quantitative evaluations and comparisons of the heat transfer rates in the absence and presence of fins are carried out.

Flow patterns

For the basic reference horizontal fluid layer with a bare plate, the layer thickness is small with respect to the plate width, the flow pattern beyond a critical value of Rayleigh number is known to be characterized by the existence of multiple convection cells [9]. In the present study, the effect of attachment of heat conducting fins to the bottom plate on the fluid flow characteristics has been investigated by examining the flow structures predicted within a single fin spacing, of aspect ratio H/S, as a function of fin height (L), fin spacing (S), and Rayleigh number (*Ra*). The flow patterns obtained within the same spacing ($H/W = H/S$) in the absence of fins ($L/H = 0.0$), have been used as reference cases for comparison.

A general picture of the effect of fin insertion on the predicted flow patterns can be inferred by comparing the number of convection cells observed in the absence and presence of fins, shown in Table 2. The numbers between brackets indicate the number of convection cells predicted using $H/W = H/S$ without fins. It can be observed from Table 2 that, in the absence of fins, the number of rotating cells is dependent upon the values of aspect ratio H/W and Rayleigh number. For the present range of Rayleigh numbers ($Ra = 2000$–$30\,000$), the predicted number of convection cells for $H/W = 0.125$, 0.25, 0.5, and 0.75 are 6–8, 4, 2, and 1, respectively. At least two Bénard convection cells have been predicted for values of $H/W \leqslant 0.5$. For higher values of H/W, the flow is characterized by the existence of a single convection cell. The intensity of this cell weakens with the increase of H/W and the decrease of Rayleigh number. Convective fluid motion have been observed to be fully suppressed, indicating pure conduction heat transfer, at $Ra = 2000$ for $H/W \geqslant 1.5$.

In the presence of fins, the number of rotating cells now depends on the values of fin spacing H/S, Rayleigh number *Ra*, and fin height L/H. A general picture of the number of cells in the presence of fins can be inferred from Table 2. Four different types of flow patterns have been observed within the fin spacing. They are distinguished by different areas shown in Table 2. Namely, a multiple-cell flow pattern (number of cells greater than 4), a two-cell flow pattern, a flow pattern with one convection cell, and a fully suppressed flow without any convective motion. For values of $H/S \leqslant 0.25$, the insertion of fins generally reduces the number of

Table 1
Grid refinement study

(a) In the absence of fins ($Ra = 3 \times 10^4$, $H/W = 0.5$)

Grid size ($N \cdot M$)	60×30	80×40	100×50	150×100	200×100
Nu	3.8459	3.8775	3.8922	3.9127	3.9121

(b) In the presence of fins ($Ra = 3 \times 10^4$, $H/S = 0.5$, $L/H = 0.5$), $N \cdot M = 100 \times 50$

NS	10	6	4	2	1
*Nu**	4.3761	4.3736	4.3724	4.3714	4.3701

Table 2
Comparison of the number of predicted convection cells in the presence and absence of fins

L/H	$Ra = 2000$			$Ra = 5000$			$Ra = 10\,000$			$Ra = 15\,000$			$Ra = 20\,000$			$Ra = 30\,000$		
	0.25	0.5	0.75	0.25	0.5	0.75	0.25	0.5	0.75	0.25	0.5	0.75	0.25	0.5	0.75	0.25	0.5	0.75
$H/S = 0.125$	8(8)	6(8)	6(8)	6(6)	6(6)	6(6)	4(6)	4(6)	4(6)	4(6)	4(6)	4(6)	4(6)	4(6)	4(6)	4(6)	4(6)	4(6)
$H/S = 0.25$	4(4)	4(4)	4(4)	4(4)	2(4)	2(4)	2(4)	2(4)	2(4)	2(4)	2(4)	2(4)	2(4)	2(4)	2(4)	2(4)	2(4)	2(4)
$H/S = 0.50$	2(2)	2(2)	2(2)	2(2)	2(2)	2(2)	2(2)	2(2)	2(2)	2(2)	2(2)	2(2)	2(2)	2(2)	2(2)	2(2)	2(2)	2(2)
$H/S = 0.75$	2(1)	2(1)	2(1)	2(1)	2(1)	2(1)	2(1)	2(1)	2(1)	2(1)	2(1)	2(1)	2(1)	2(1)	2(1)	2(1)	2(1)	2(1)
$H/S = 1.00$	2(1)	2(1)	2(1)	2(1)	2(1)	2(1)	2(1)	2(1)	2(1)	2(1)	2(1)	2(1)	2(1)	2(1)	2(1)	2(1)	2(1)	2(1)
$H/S = 1.25$	2(1)	2(1)	2(1)	1(1)	2(1)	2(1)	2(1)	2(1)	2(1)	2(1)	2(1)	2(1)	2(1)	2(1)	2(1)	2(1)	2(1)	2(1)
$H/S = 1.50$	0(0)	0(0)	0(0)	1(1)	2(1)	2(1)	1(1)	2(1)	2(1)	2(1)	2(1)	2(1)	2(1)	2(1)	2(1)	2(1)	2(1)	2(1)
$H/S = 1.75$	0(0)	0(0)	0(0)	1(1)	0(1)	0(1)	1(1)	2(1)	2(1)	1(1)	1(1)	2(1)	1(1)	2(1)	2(1)	1(1)	2(1)	2(1)
$H/S = 2.00$	0(0)	0(0)	0(0)	1(1)	0(1)	0(1)	1(1)	1(1)	2(1)	1(1)	1(1)	2(1)	1(1)	1(1)	2(1)	1(1)	1(1)	2(1)

Multiple cells Two cells One cell Suppressed flow

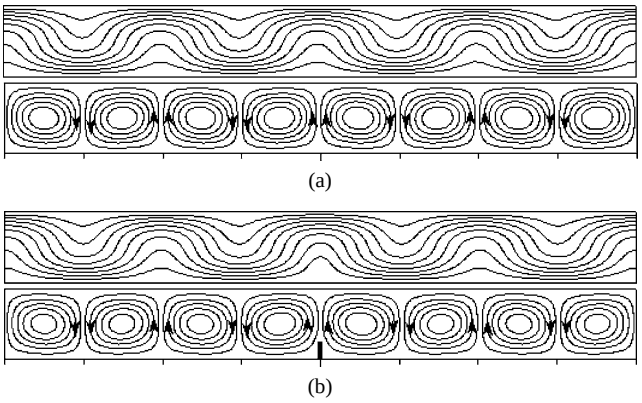

Fig. 2. (a) Streamlines and isotherms without fins ($Ra = 2000$, $H/W = 0.125$). (b) Streamlines and isotherms using fins ($Ra = 2000$, $H/S = 0.125$, $L/H = 0.25$).

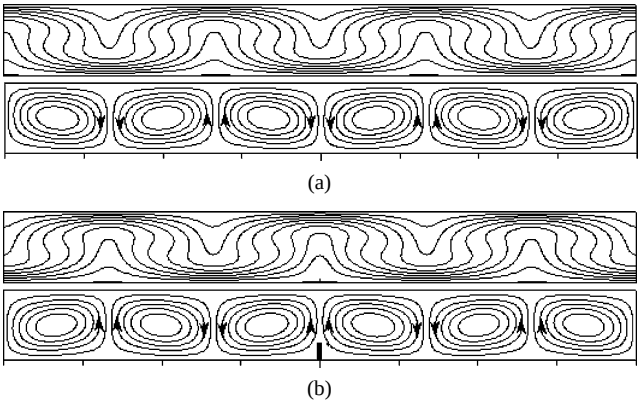

Fig. 3. (a) Streamlines and isotherms without fins ($Ra = 5000$, $H/W = 0.125$). (b) Streamlines and isotherms using fins ($Ra = 5000$, $H/S = 0.125$, $L/H = 0.25$).

convection cells as compared to the reference case of a bare plate. Two-cell convection patterns have been observed both in the absence and presence of fins for values of $H/S = 0.5$. On the other hand, for values of $H/S = 0.75$–1.25, the insertion of fins results in inducing a two-cell convection pattern as compared to single cell in the absence of fins. The range of predicted two-cell flow pattern is extended in comparison with the bare plate. For low values of fin spacing ($H/S \geqslant 1.5$), the predicted number of convection cells is largely dependent upon the values of fin height and Rayleigh number. In comparison with the prediction of a single cell in the reference case of a bare plate, the insertion of fins may result in developing a two-cell convection pattern, a single-cell convection pattern, or completely suppress the fluid motion.

The foregoing comparison between the flow patterns in the presence and absence of fins is general. A more detailed comparison can be made by comparing the flow streamlines and isotherms for the two cases and for equivalent number of flow cells and domain aspect ratio. Fig. 2(a), (b) shows a typical flow pattern that is characterized by eight rotating cells. The streamlines and isotherms with and without fins are completely similar. The insertion of heat conducting fin induces an upward fluid motion along the fin walls that happens to be in the same direction as the original fluid motion without fins. It can be also observed from Fig. 2 that, closely spaced isotherms at the top and bottom plates correspond to the locations of fluid impingement on these plates. These locations are characterised by high local values of heat transfer rates. The increase of Rayleigh number results in higher temperature gradients at these locations and consequent higher values of local heat transfer coefficients.

For values of $H/S = 0.125$, $L/H > 0.25$, and $Ra = 2000$–5000, the flow pattern is characterised by the existence of six rotating cells. Comparison of this flow pattern with the basic six rotating cells flow pattern obtained without fins is shown in Fig. 3(a), (b). It can be observed that, although the number of cells is the same, the cells orientation and direction of rotation are reversed as due to the insertion of

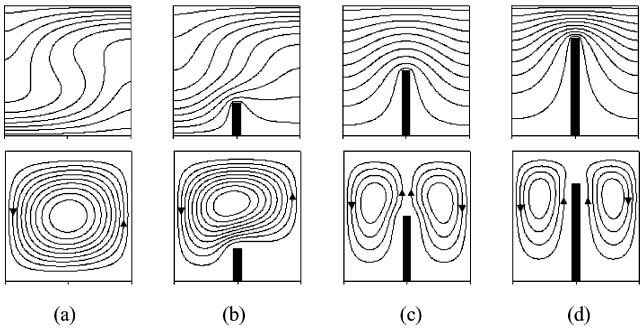

Fig. 4. Streamlines and isotherms, $Ra = 5000$, $H/S = 1.25$: (a) Without fin, (b) $L/H = 0.25$, (c) $L/H = 0.5$, (d) $L/H = 0.75$.

fins. Again, the insertion of heat conducting fin induces an upward fluid motion along the fin walls. The streamlines and isotherms of Fig. 3(a) can be considered as a mirror image of those shown in Fig. 3(b). The locations of condensed isotherms and corresponding peaks in local heat transfer coefficient have exchanged their positions between the hot and cold plates.

Further comparisons of the four-cell and two-cell flow patterns in the absence and presence of fins have been carried out. It has been observed that, the four-cell flow patterns are similar in the presence and absence of fins. On the other hand, the cells orientation and direction of rotation in the two-cell flow pattern using fins have been observed to be opposite to the basic two-cell flow patterns predicted in the absence of fins.

Streamlines and isotherms corresponding to a single-cell flow pattern are shown in Fig. 4(a), (b). The transition from single to two-cell flow patterns with the increase of fin height at the same value of Rayleigh number is also shown in Fig. 4(c), (d). It can be observed that the convection cells move outward away from the fin surface with the increase of fin height. Also, the temperature gradient at the cold plate above the fin tip increases with the increase of fin height.

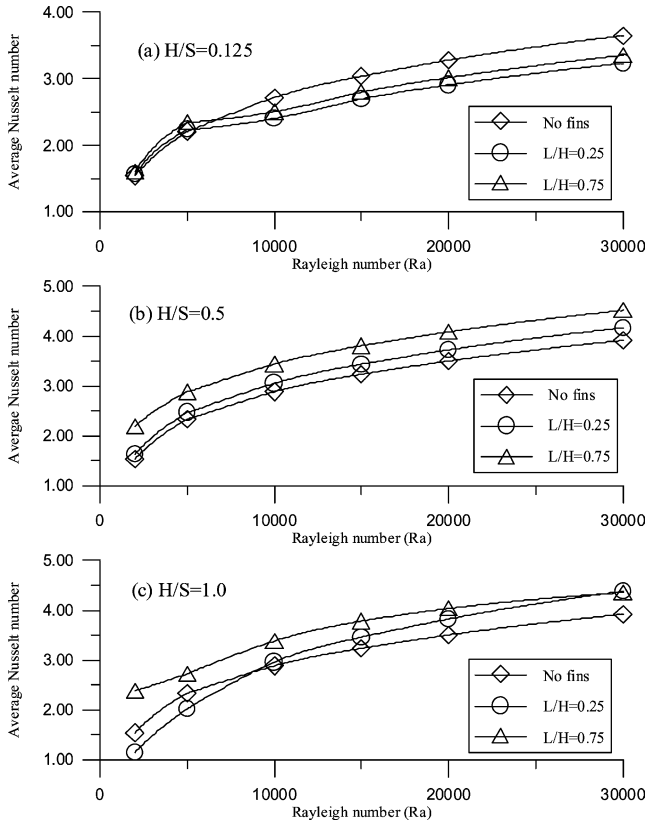

Fig. 5. Variation of average value of heat transfer Nusselt number from a single fin spacing Nu^* with Rayleigh number for different values of fin height: (a) $H/S = 0.125$, (b) $H/S = 0.5$, and (c) $H/S = 1.0$.

Heat transfer rates

Analysis of the effect of fin insertion on the heat transfer rates from a horizontal fluid layer should clarify two points. The first one, is related to the comparison of heat transfer rates from a single fin spacing (of aspect ratio H/S) with the corresponding values obtained within the same spacing ($H/W = H/S$) in the absence of fins. The second issue is related to the variation of heat transfer rates and finned surface effectiveness as a function of Rayleigh number, fin spacing H/S, and fin height L/H. The results of this analysis are useful in the design of finned surface to maximize the heat transfer rates and optimize the cost of fin material for a particular application.

Fig. 5(a)–(c) shows the variation of average value of heat transfer Nusselt number from a single fin spacing (Nu^*) with Rayleigh number for different values of fin height. These values are compared to the average Nusselt number values (Nu) obtained for the same spacing ($H/W = H/S$) in the absence of fins, also shown in Fig. 5. The values of H/S chosen for this comparison ($H/S = 0.125$, 0.5, and 1.0) represent three different cases of predicted flow patterns, see Table 2. It can be observed from Fig. 5(a) that for $H/S = 0.125$, the heat transfer rates generally decrease with fin insertion. This may be mainly attributed to the reduction in the number of flow rotating cells and corresponding local peaks of heat transfer rates. For fin spacing of $H/S = 0.5$, the flow pattern is characterized by the existence of two convection cells both in the absence and presence of fins. The decrease in flow intensity with fin insertion is not significant. The insertion of fins for this case results in relatively higher values of heat transfer rates, as shown in Fig. 5(b). The heat transfer rates increase with the increase fin height.

Analysis of the variation of heat transfer rates with Rayleigh number for $H/S = 1.0$, see Fig. 5(c), indicates that the heat transfer rates are reduced at low values of fin height and Rayleigh number ($L/H = 0.25$, $Ra = 2000$–5000) as compared to the basic case without fins. It should be mentioned that, the number of convection cells within this range are the same in absence and presence of fins, see Table 2. The reduction of heat transfer rates is attributed to the decrease in flow intensity due to the insertion of fins. The heat transfer rates have been observed to be enhanced for this case ($H/S = 1.0$, $L/H = 0.25$) with the increase of Rayleigh number. For high values of fin height ($L/H = 0.75$), the heat transfer rates using fins are relatively higher than the corresponding values in the absence of fins for all values of Rayleigh number.

The above results show that the heat transfer rates are largely dependent upon the competition between the effects of increase of heat transfer surface area, the reduction or increase of the number of convection cells, and the variation of flow intensity as due to the insertion of fins. The complex interactions between these parameters determine the resulting heat transfer rates. In actual applications, the general design requirement is to maximize and enhance the total heat transfer rate and finned surface effectiveness with the insertion of fins. However, in some situations, one may be interested in maximizing the heat transfer rates at a particular location from single fin spacing on the hot plate. That is characterized, for example, by relatively high heat dissipation rates to avoid the possibility of hot spots at these points. The variation of the heat transfer rates and finned surface effectiveness from a horizontal fluid layer with bottom plate finned surface as a function of fin spacing H/S, for different values of Rayleigh number and fin height L/H are discussed in the following sections.

The variation of the average value of Nusselt number (Nu^*) from the finned surface with fin spacing H/S for different values of fin height and Rayleigh number is shown in Fig. 6(a)–(c). The maximum value of heat transfer rate from a single fin spacing occurs at bout $H/S = 0.5$–0.75. For high values of fin height ($L/H = 0.75$) and low Rayleigh number, conduction heat transfer dominates and the heat transfer rate from a single spacing increases linearly, as expected, with the decrease of fin spacing.

In actual design of finned surface, the layer aspect ratio is known and the designer seeks to calculate the finned surface effectiveness using a particular value of fin height (L/H) and spacing (H/S) for a given temperature difference (Ra). It should be noted that, calculation of the fin effectiveness

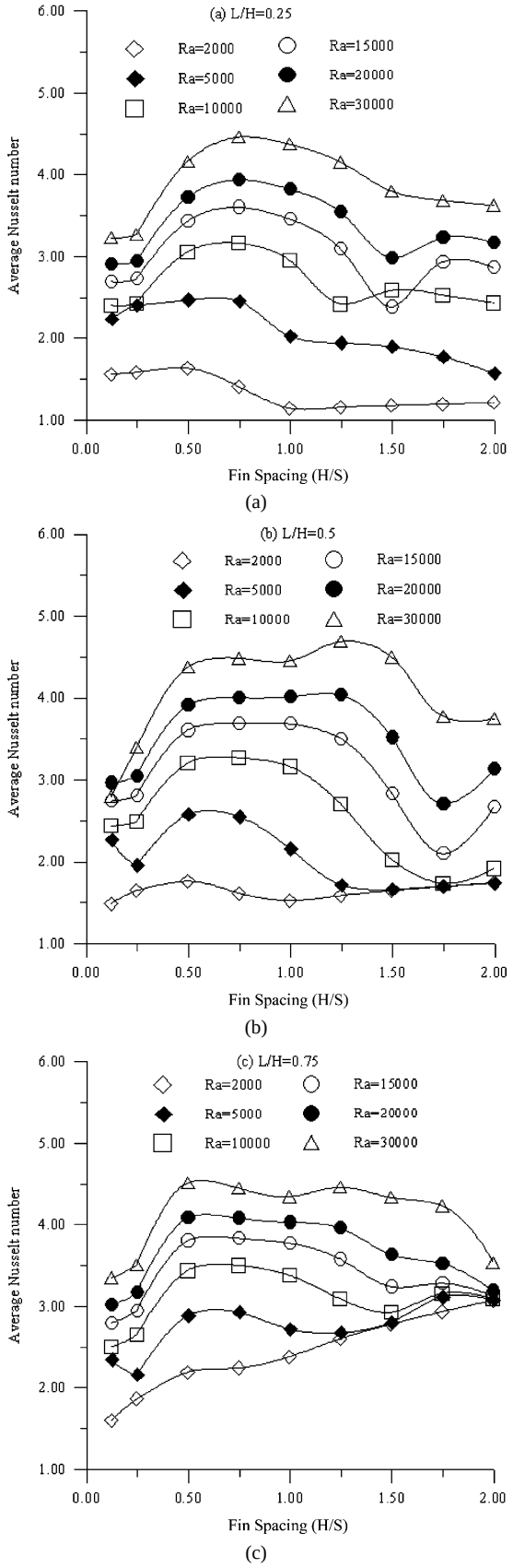

Fig. 6. Variation of average value of heat transfer Nusselt number from a single fin spacing Nu^* as function of fin spacing (H/S) and Rayleigh number: (a) $L/H = 0.25$. (b) $L/H = 0.5$. (c) $L/H = 0.75$.

using Eq. (10) requires specification of the reference value of heat transfer Nusselt number Nu in the absence of fins. In the present study, the thickness of the basic reference horizontal fluid layer with bared plate is considered to be small with respect to the layer width. The corresponding convection patterns are known to be characterized by the existence of multiple convection cells. These convection patterns have been observed in the present study for values of $H/W \leqslant 0.5$. The variation of heat transfer Nusselt number with Rayleigh number for $H/W \leqslant 0.5$ has been correlated as:

$$Nu = 0.1225(Ra)^{0.3395} \tag{11}$$

The Nusselt number value obtained from Eq. (11) has been taken as reference in the calculation of total finned surface effectiveness.

The variation of total finned surface effectiveness with fin spacing for different values of fin height and Rayleigh number is shown in Fig. 7(a)–(c). Values of fin effectiveness greater than one indicate an enhancement of heat transfer using fins. For the present range of Rayleigh number, the effectiveness of the finned surface is a strong function of fin spacing and height. The finned surface effectiveness increases with the increase of fin height. Low values of fin height may result in reducing the heat transfer rates as compared to a bare plate. For enhancing the heat transfer rates, the fin spacing for low values of fin height should be carefully chosen as a function of Rayleigh number.

For high values of fin height ($L/H \geqslant 0.75$), Fig. 7(c), the finned surface effectiveness is greater than one, for a wide range of fin spacing. The dependence of finned surface effectiveness on the Rayleigh number value is decreased. A fin spacing of $H/S = 0.5$–0.75 seems to be an optimum value for maximum finned surface effectiveness. For low values of Rayleigh number and high values of fin height, the finned surface effectiveness increases linearly with the decrease of fin spacing.

The above results have been obtained for a single value of fin thickness ($t_f/H = 0.05$). For the completeness of the present study, the effect of variation of fin thickness on the heat transfer rates has been examined. The average values of heat transfer Nusselt number for three different values of fin thickness $t_f/H = 0.05$, 0.025, and 0.0125 (at $Ra = 30\,000$, $L/H = 0.5$, and $H/S = 0.5$) have been respectively predicted as 4.376, 4.407, and 4.420. These results indicate a very slight enhancement in the heat transfer rates with decreasing the value of fin thickness. In practice, the choice of fin thickness is carried out based on the manufacturing capability to produce as thin fins as possible.

Useful guidelines

The following guidelines are recommended for practical applications:

- The total finned surface effectiveness is generally enhanced for the following design ranges: ($L/H = 0.75$

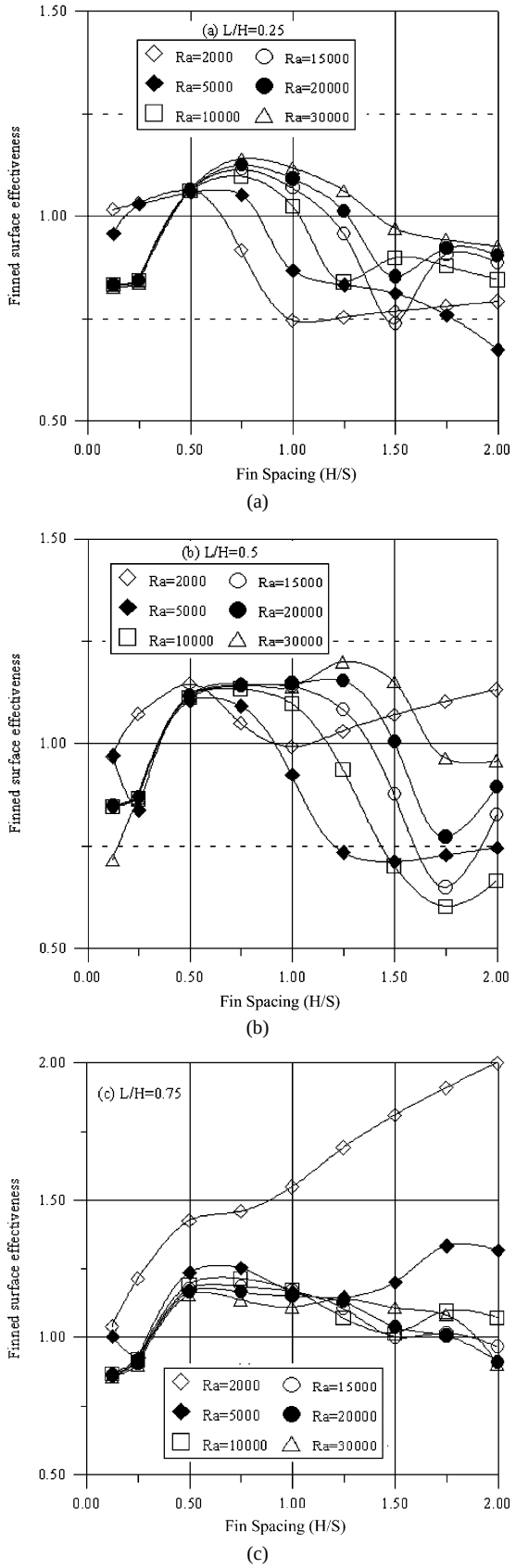

Fig. 7. Variation of total finned surface effectiveness ($\varepsilon_f = Nu^*/Nu$) with fin spacing, $Nu = 0.1225(Ra)^{0.3395}$: (a) $L/H = 0.25$, (b) $L/H = 0.5$, (c) $L/H = 0.75$.

and $H/S = 0.5$–1.5), ($L/H = 0.5$ and $H/S = 0.5$–0.75), and ($L/H = 0.25$ and $H/S = 0.5$).

- For values outside these ranges, the fin design parameters should be carefully chosen as function of the Rayleigh number value, using Fig. 7(a)–(c).
- The heat transfer rate from a single fin spacing is optimised for values of $H/S = 0.5$–0.75.
- The heat transfer rates increase by using higher values of fin height.
- The fin thickness is determined by the manufacturing limitations of thin fins production.

7. Summary and conclusion

Numerical experiments have been carried out to investigate heat transfer and fluid flow characteristics from a horizontal fluid layer with finned bottom surface. Results of heat transfer and fluid flow from the finned surface have been compared with the base case of bare plate. The effects of fin height ($L/H = 0.25$, 0.5, and 0.75) and fin spacing ($H/S = 0.125$–2.0) have been investigated for a wide range of Rayleigh numbers ($Ra = 2000$–$30\,000$). Quantitative comparisons of heat transfer rates and finned surface effectiveness have been reported. The insertion of heat conducting fin induces an upward fluid motion along the fin walls. Four different types of flow patterns have been predicted within the fin spacing as function of the values of fin height and Rayleigh number. Namely, a multiple-cell flow pattern (number of cells greater than 4), a two-cell flow pattern, a flow pattern with one convection cell, and a fully suppressed flow without any convective motion.

The maximum value of heat transfer rate from a single fin spacing occurs at bout $H/S = 0.5$–0.75. For the present range of Rayleigh number, the effectiveness of the finned surface is a strong function of fin spacing and height. The finned surface effectiveness increases with the increase of fin height. Low values of fin height may result in reducing the heat transfer rates as compared to a bare plate. For enhancing the heat transfer rates, the fin spacing for low values of fin height should be carefully chosen as a function of Rayleigh number.

For high values of fin height ($L/H \geqslant 0.75$), the finned surface effectiveness is greater than one, for a wide range of fin spacing. The dependence of finned surface effectiveness on the Rayleigh number value is decreased. A fin spacing of $H/S = 0.5$–0.75 seems to be an optimum value for maximum finned surface effectiveness. For low values of Rayleigh number and high values of fin height, the finned surface effectiveness increases linearly with the decrease of fin spacing.

References

[1] K.E. Starner, H.N. McManus, An experimental investigation of free convection heat transfer from rectangular fin-arrays, J. Heat Transfer (1963) 273–278.
[2] J.R. Welling, C.B. Wooldridge, Free convection heat transfer coefficient from rectangular vertical fins, J. Heat Transfer (1965) 439–444.
[3] F. Harahap, H.N. McManus, Natural convection heat transfer from horizontal rectangular fin arrays, J. Heat Transfer (1967) 32–38.
[4] C.D. Jones, L.F. Smith, Optimum arrangement of rectangular fins o, horizontal surfaces for free convection heat transfer, J. Heat Transfer (1970) 6–10.
[5] A. Bar-Cohen, Fin thickness for an optimized natural convection array of rectangular fins, J. Heat Transfer (1979) 564–566.
[6] E.M. Sparrow, C. Prakash, Enhancement of natural convection heat transfer by a staggered array of discrete vertical plates, J. Heat Transfer (1980) 215–220.
[7] H. Yüncü, G. Anbar, An experimental investigation on performance of rectangular fins on a horizontal base in free convection heat transfer, Heat Mass Transfer 33 (1998) 507–514.
[8] A. Güvenc, H. Yüncü, An experimental investigation on performance of rectangular fins on a vertical base in free convection heat transfer, Heat Mass Transfer 37 (2001) 409–416.
[9] G.D. Raithby, K.G.T. Holland, Natural convection, in: W.M. Rosenhow, J.P. Hartnett, E.N. Ganic (Eds.), Handbook of Heat Transfer Fundamentals, second ed., McGraw-Hill, New York, 1985, Chapter 6.
[10] D. Mukutmoni, K.T. Yang, Rayleigh–Bénard convection in a small aspect ratio enclosure, Part I—Bifurcation to oscillatory convection, J. Heat Transfer 115 (1993) 360–366.
[11] D. Mukutmoni, K.T. Yang, Rayleigh–Bénard convection in a small aspect ratio enclosure, Part II—Bifurcation to chaos, J. Heat Transfer 115 (1993) 367–376.
[12] D. Mukutmoni, K.T. Yang, Thermal convection in small enclosures: An atypical bifurcation sequence, Internat. J. Heat Mass Transfer 38 (1995) 113–126.
[13] K.T. Yang, Transitions and bifurcations in laminar buoyant flows in confined enclosures, J. Heat Transfer 110 (1988) 1191–1204.
[14] A.Y. Gelfgat, Different modes of Rayleigh–Bénard instability in two- and three-dimensional rectangular enclosures, J. Comput. Phys. 156 (1999) 300–324.
[15] S. Inada, T. Taguchi, W.-J. Yang, Effects of vertical fins on local heat transfer performance in a horizontal fluid layer, Internat. J. Heat Mass Transfer 42 (1999) 2897–2903.
[16] S.V. Patankar, Numerical Heat Transfer and Fluid Flow, Hemisphere, New York, 1980.
[17] Aquilon, Logiciel de modélisation en mécanique des fluides et transferts, TREFLE-ENSCPB, http://www.enscpb.fr/master/Aquilon/index.htm.
[18] M. Fortin, R. Glowinski, Méthode de Lagrangien Augmenté. Application à la Résolution Numérique des Problèmes aux Limites, in: Collection Méthodes Mathématiques de l'Informatique, Dunod, Paris, 1982.